geosciences

MDPI

Article

Southern Hemisphere Pressure Relationships during the 20th Century: Implications for Climate Reconstructions and Model Evaluation

Logan Clark [1] and Ryan Fogt [2]

[1] Department of Geography, Ohio University, Athens, OH 45701, USA; lc491313@ohio.edu
[2] Department of Geography, Ohio University, Athens, OH 45701, USA; fogtr@ohio.edu

Abstract:

The relationship between Southern Hemisphere mid and high-latitude regions have made it possible to extend observation-based pressure reconstructions back throughout the 20th century to understand Antarctic climate behavior, even though routinely collected observations for this continent only began around 1957. Reconstructions inherently assume stability in these relationships through time, and this stationarity constraint can be fully tested in a model setting. Seasonal pressure reconstructions based on the principal component regression (PRC) method spanning 1905 – 2013 are done entirely within the framework of the Community Atmospheric version 5 (CAM5) model here, and evaluated to the observation-based reconstructions in Fogt [1] to assess the overall skill. The CAM5 'best' reconstructions performed better in every season comparatively expect in the austral summer (DJF), with nearly every model experiment exhibiting larger anomalies (in an absolute sense) compared to the station-based reconstructions. The stationarity constrained when tested in a number of ways appeared remain fairly stable, with only weaker stability noted at Esperanza station, as well as in the austral summer, thought to be driven by the prescribed SST forcings within CAM5. The weaker summer skill in our model reconstructions was a manifestation of fewer midlatitude stations (predictors) used when creating the reconstruction, which shows that the number of predictors utilized in the reconstruction correlates well in overall skill.

Keywords: Antarctica, pressure, variability, model evaluation, climate change

1. Introduction

The Southern Annular Mode (SAM) characterizes relationships between the pressure across Antarctica and the pressure in the southern midlatitudes[2,3]. In particular, the SAM represents the strength of the pressure gradient across the extratropical Southern Hemisphere (SH) and associated strength of the SH westerly jet [4]. As the dominant mode of SH climate variability[3,5,6], the SAM explains ~20-35% of total Southern Hemisphere monthly atmospheric circulation variability from daily [7] to decadal timescales [8]. Other hemispheric-scale coupled ocean-atmospheric circulation patterns such as the El Niño-Southern Oscillation (ENSO [9]), the Pacific Decadal Oscillation [10] / Interdecadal Pacific Oscillation [11], and the Atlantic Multidecadal Oscillation [12] connect tropical sea surface temperature variations to Antarctica climate variations via teleconnections associated with tropically-generated Rossby Waves **[13–19]**. Unsurprisingly, modeling and observational studies note that tropical variability can also influence the state of the SAM **[20–25]**, adding layers of complexity to the connections Antarctica shares with the SH climate.

Nonetheless, utilizing the relationships between the extrapolar regions of the SH with Antarctica has allowed for numerous observation-based reconstructions of Antarctic climate. In particular, SAM indices have been generated throughout the 20th century based on mid-latitude pressure observations **[26–28]**. Indeed, in his SAM index reconstruction, Visbeck [28] assumed that changes in Antarctic pressure were directly proportional to those changes in the midlatitudes. As an extension of SAM index reconstructions, the relationship between pressure in the SH mid-latitudes with Antarctica was further employed to reconstruct seasonal mean pressure observations at 18 Antarctic stations back to 1905 [1,29].

While all of these reconstructions add value in understanding historical pressure variability across Antarctica throughout the 20th century, they all are based on a similar underlying assumption. This premise, called the stationarity constraint, is common in nearly all climate reconstructions, and assumes that the relationships between the predictor data (in this case, mid-latitude pressure observations) and the reconstructed climate variable (SAM index or Antarctic pressure observation) remain the same throughout time as they are during the reconstruction calibration period [30]. However, without long-term continuous measurements of the reconstructed variable, the accuracy of this stationarity constraint is nearly impossible to fully assess.

Apart from reconstructions, climate model experiments are important tools for understanding historical Antarctic climate, and for example have been used to evaluate the effect of the SAM on Antarctic temperature [31], West Antarctic climate variability [32], and Antarctic pressure [33,34]. However, the reliability of climate models in accurately representing Antarctic climate is again challenging to fully determine, as comparison with observations can only be made since 1957, and even shorter for Antarctic sea ice [35]. Given the combination of large interannual variability and the relatively short length of Antarctic climate variations, detection and attribution of change in both observations and models is difficult [36]. As such, Bracegirdle et al. [37] reiterate the importance of developing longer-term datasets to help quantify the degree to which a climate model may over- or under-estimate responses to various climate forcings in the past, which in turn would understand its biases in future projections. This is especially true since other long-term estimates of Antarctic climate variability from gridded reanalyses have been shown to be of lower quality in the early 20th century, directly tied to the quantity of observations assimilated in the reanalyses [38]; there are even notable jumps in the performance of 20th century reanalyses after 1957 for Antarctic pressure [39].

In this study, we provide an alternate form of climate model evaluation as well as a better assessment of the stationary constraint assumed in previous Antarctic climate pressure reconstructions based on statistical relationships with mid-latitude pressure. This evaluation is entirely done within the framework of the Community Atmospheric Model version 5 (CAM5) model. There are multiple benefits of using a non-coupled climate model to perform these evaluations. First, unlike the reanalyses, CAM5 is based only on the prescribed forcing mechanisms, and is therefore not sensitive to changes in quantity of observations [38]. Second, it is a continuous dataset, allowing us to fully examine changes in the strength of the pressure relationship between the mid and high latitudes of the SH, and better quantify the overall reconstruction skill (since direct data withheld outside a calibration window in the model can be used for comparison). Second, using multiple experiments as in previous work [33,34] allows to determine if any particular prescribed forcing mechanisms significantly influence the mid-to-high latitude SH pressure relationships. Finally, the evaluation can also be thought of as another version of model assessment, in particular when comparing differences in the strength of the relationships between mid and high latitudes pressure over the SH in the model compared to observations.

This paper is structured as follows. The following section describes the data and methods of our study, including more details on the CAM5 model and the procedure for creating the reconstructed pressure datasets. Section 3 analyzes the pressure relationships between the mid and high latitudes of the SH through evaluating the reconstructions in the CAM5 model, and describes differences compared to previous work that are related to various forcing mechanisms, model biases, or violations of the stationarity assumption. Section 4 summarize some of the major conclusions / results found in this study as well as their implication for both climate model assessment and future Antarctic climate reconstructions based on midlatitude data.

2. Data and Methods

2.1 CAM5

The National Center for Atmospheric Research (NCAR) Community Atmospheric Model version 5 (CAM5) is configured at a 0.9° latitude x 1.25° longitude horizontal resolution, with a finite volume dynamical core and 26 vertical levels [33]. CAM5 is a non-coupled atmosphere-only climate model, and three experiments spanning the entire 20th century are analyzed to help isolate the sensitivity of various external forcings as in earlier work [33,34]. In addition, each experiment is comprised of 10 ensemble members, each initialized with a random perturbation in air temperature. The first experiment will be termed "Ozone Only," in which ozone concentrations vary over time (1900 – 2014), whereas SSTs, sea ice concentrations and non-ozone radiative forcings are held to their monthly repeating climatologies. The second experiment is termed "Tropical SSTs + Fixed Radiative," with only time-varying tropical SSTs (1874 – 2014) prescribed; all other forcings are held to their monthly climatologies in this simulation. The third experiment is termed "Tropical SSTs + Radiative," in which time-varying tropical SSTs and radiative forcings (1880 – 2014) are combined [33]. A list of these experiments can be found in Table 1 below.

CAM5 Experiment	Time Period (Years)	Forcing(s)
1. Ozone Only	1990 – 2014	Ozone (O_3) Time-varying ozone concentrations
2. Tropical SSTs + Fixed Radiative	1874 – 2014	SSTs (28°N - 28°S) Time-varying tropical SSTs
3. Tropical SSTs + Radiative	1880 – 2014	SSTs (28°N - 28°S) Time-varying tropical SSTs and all radiative forcings

Table 1. List of CAM5 model experiments, their available time periods, and external forcing mechanisms that characterize each experiment.

2.2 Gridded Global Reanalyses

For comparison, mean sea level pressure is also evaluated across the Southern Hemisphere in various 20th century reanalyses. The project was designed to yield an atmospheric circulation

dataset that's only assimilating direct surface pressure observations, leaving monthly SSTs and sea-ice concentrations as the boundary conditions. The three century-length reanalysis datasets that will be evaluated here include the National Oceanic and Atmospheric Administration / Cooperative Institute for Research in Environmental studies (NOAA-CIRES) 20th Century reanalysis (20CR) version 2 [40], the European Center for Medium Range Forecasting (ECMWF) 20th Century reanalysis (ERA-20C) [41], and ECMWF's Coupled Ocean-Atmosphere Reanalysis of the 20th Century (CERA-20C) [42]. The CERA-20C product is the newest reanalysis that was designed to mitigate some of the flaws observed in ERA-20C [42], with the additive of ocean temperature and salinity from version 4 of the Met Office Hadley Centre (EN4). Each of these three products assimilate their surface pressure observations from the International Surface Pressure Databank (ISPD) [43], but ERA-20C and CERA-20C also assimilate marine surface from the International Comprehensive Ocean-Atmosphere Data Set (ICOADS) [44]. As 20CR and CERA-20C are ensemble reanalyses, we use the ensemble mean MSLP as the best representation of pressure across Antarctica throughout the 20th century.

In addition to the century-length reanalyses, the ECMWF interim reanalysis (ERA-Interim) dataset will be used to compare against our reconstructions. While this dataset only extends back to 1979, previous studies deemed its exceptional reliability for mean sea-level pressure (MSLP) [45],[46]. This allows for another reliable dataset used for comparison / evaluation of observed differences between the reconstructions and reanalyses.

2.3 PCR Reconstruction Procedure and Validation

Principal Component Regression (PCR) will be used in similar fashion in previous SAM index and Antarctica pressure observation reconstructions [1,27], but instead done entirely within the CAM5 model. In this case, the 29 midlatitude stations, represented as the closest gridpoint in CAM5, are used to predict (reconstruct) pressure at select Antarctic stations (also the closest gridpoints in CAM5). Prior to performing PCR, the first step in this process involves correlating the midlatitude stations to Antarctic stations within the model. Then, only the stations that are significantly correlated at $p < 0.05$ and $p < 0.10$ (5% and 10% networks respectively), are selected. Principal Component Analysis (PCA) is performed on the subset of midlatitude stations that are significantly correlated to Antarctica, known as the predictors. PCA produces a set of principal components (i.e. timeseries), where again only a subset of these components are chosen that represent significant correlations at the 5% and 10% networks. PCA becomes superior to multiple linear regression from this previously mentioned step as only using a subset of principal components acts as a sort of noise reduction, whereby only the midlatitude stations that explain a large portion of the variance are used. The final step in this procedure involves regressing the subset of principal components onto the Antarctic stations, in which the regression coefficients from

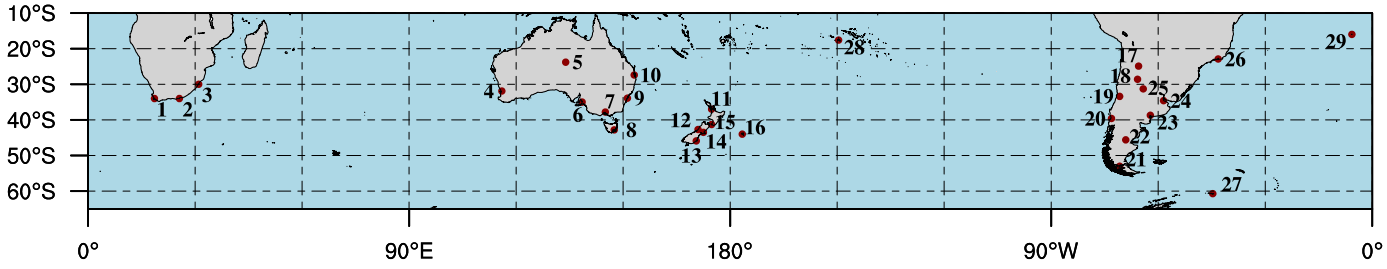

1. Cape Town	6. Adelaide	11. Auckland	16. Chatham Island	21. Punta Arenas	26. Rio de Janeiro
2. Port Elizabeth	7. Melbourne	12. Hokitika	17. Salta	22. Sarmiento	27. Orcadas
3. Durban	8. Hobart	13. Dunedin	18. Catamarca	23. Bahia Blanca	28. Tahiti
4. Perth	9. Sydney	14. Christchurch	19. Santiago	24. Buenos Aires	29. St. Helena Island
5. Alice Springs	10. Brisbane	15. Wellington	20. Valdivia	25. Cordoba	

the midlatitudes can ultimately be used to reconstruct pressure at a single gridpoint. This PCR method is repeated for each Antarctic station that was done for the Fogt [1] observation-based reconstructions, as well as every experiment / ensemble member within CAM5. Additional reconstructions will be created where trends are already present within the PCR model (trended dataset), and where the fitting in the PCR method is based on completely detrended data (detrended dataset) prior to creating the reconstruction. All of these reconstructions and figures to follow will be made using the NCAR Command Language (NCL) program. A map of the 29 midlatitude stations used as predictor data in the CAM5 model for the reconstruction procedure can be seen in Figure 1 below.

Figure 1. Map and list of names of the 29 midlatitude stations used in the study as the gridpoint locations in CAM5 for performing the PCR reconstruction method.

Validation techniques such as calibration and validation correlations, reduction of error (RE), and coefficient of efficiency (CE) will be used to assess the skill of the model-based seasonal reconstructions. Calibration correlation is calculated by comparing the reconstructed CAM5 pressure dataset to the original pressure data within CAM5, which helps to evaluate their linear relationship. The full length of the pressure reconstructions will span 1905 – 2013, with the same calibration period of 1957 – 2013 to precisely match previous work [1]. However, the validation period that is responsible for producing our validation correlation is different from previous work. Based on the 'full' reconstructions of Fogt et al. [1], the validation period was also 1957-2013, and a leave-one-out cross validation procedure was employed to generate an independent validation timeseries. Here, since the model data are continuous throughout the entire 20th century, the validation period is prescribed to be the 1905 – 1956 time period, and the reconstructed data during this time can be independently evaluated to the original CAM5 data as a more robust method of evaluating the reconstruction. Given this difference in validation periods and approaches, and the fact that the skill metrics of validation correlation and CE are based on comparison of the actual data with the validation timeseries, there will be some differences arising in these metrics compared to Fogt et al. [1]. Nonetheless, the approach here where the calibrated period will be used to predict the pressure over the independent validation period serves as an additional means of testing the robustness of the PCR procedure for generating pressure reconstructions (i.e. validation correlation). RE and CE skill metrics are used to further test the reliability of the calibration and validation reconstructions, respectively. These statistics indicate whether the model-based reconstructions are able to outperform the climatological average for pressure, with the range of values extending from -∞ to positive 1.0. Anything greater than 0.0 thus indicates that the model reconstructions (both calibrated and validated) outperform the climatological average for pressure.

3. Results

3.1 Reconstruction Performance

As noted before, CAM5 reconstructions were created across the 5% and 10% skill networks, along with using an original and completely detrended dataset. Across all of these skill metrics and the ten CAM5 ensemble members, the 'best' reconstructions values were chosen and plotted seasonally by experiment, along with the best observational reconstruction values from Fogt et al. [1], shown in Figure 2. Best reconstructions from the CAM5 data were chosen based on the highest calibration / validation correlations, RE and CE values by station, across all ten ensemble members. By doing this, every single Antarctic station and season will have a different ensemble member and skill network (5% or 10%) associated with it depending on their performance during the full 1905 – 2013 time period. This allows us to understand how the best performing CAM5 ensembles and networks reconstruct pressure through time at different Antarctic station locations, and what the best skill ultimately looks like.

Overall, it was found that the highest skill across all CAM5 experiments is during the austral winter (JJA), while the observation-based reconstruction from Fogt et al. [1] performs the best in the austral summer (DJF), with JJA being the second best season for that dataset. Both the spring (SON) and fall (MAM) seasons exhibit weaker skill between all datasets, but the model does tend to outperform the observational reconstruction in every season with the exception of DJF. This is worth noting, especially due to the fact that the model has an independent validation period (1905 – 1957) that doesn't appear to reduce overall performance with any CAM5 experiment. All CAM5 experiments, as well as the observational reconstruction, generally remain above 0.5 for both calibration and validation correlation, with RE and CE never dropping below 0.0. Since every skill metric remains positive, the model-based reconstructions created here are thus more reliant than using the climatological average for pressure when examining long-term variability.

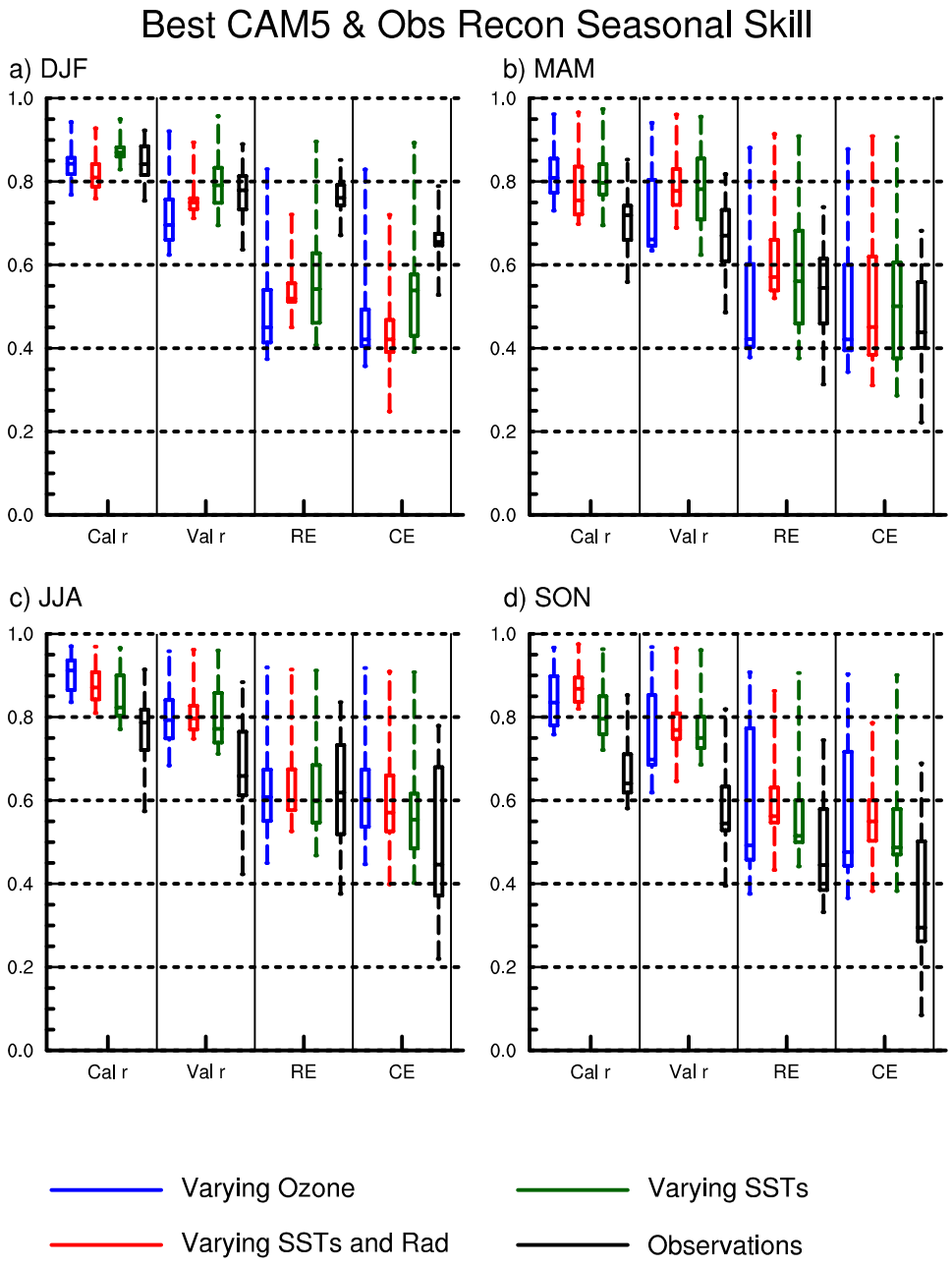

Figure 2. Best CAM5 seasonal reconstruction values across 5%, 10%, trended and detrended networks within each experiment. Best observation-based reconstruction values also added in [1], with skill metrics of calibration / validation correlation, RE and CE plotted. All datasets are evaluated over the 1905 – 2013 time period.

To further evaluate the 'best' model-based reconstruction, a timeseries of seasonal station-based pressure anomalies is plotted against the observation-based reconstruction, as well as the original CAM5 dataset that was used to produce the modeled reconstructions. CAM5 reconstructions display larger pressure anomalies in MAM and SON, primarily during the first half of the 20th century. Some of the greatest discrepancies between the two reconstructed datasets appears at Esperanza in SON, where both the CAM5 original and reconstructed datasets show pressure anomalies above 11 hPa around 1910, which is in stark contrast to observations which display near-zero and even negative pressure anomalies around that same timeframe. These large anomalies spawned from the 9th ensemble member and the 5% network at Esperanza in SON, which goes to show that even though it was chosen as the best reconstruction timeseries, there are clearly notable differences between the model and observations during this season. Overall, the CAM5 datasets (all experiments) typically display larger pressure anomalies (in an absolute sense) for all seasons when compared to the observational reconstruction, which may be driven by the prescribed external forcings within the models framework.

Correlations between all three datasets were also calculated and listed at the top of each plot to provide a fixed value in directly comparing these data over the 1905 – 2013 time period. It is interesting to see that negative correlation values between our model reconstructions and observation-based reconstructions appear a number of times in all seasons except for JJA. Even though JJA remains above 0.0 when correlating the model reconstruction to the observation-based reconstruction, the highest value still only remains at ~ 0.03. Indeed, the lowest correlation is observed at Esperanza in SON with a correlation of -0.16 between the model and observation reconstruction, and -0.17 between the original CAM5 data and the observation reconstruction. While DJF appears to have the highest correlation values, these correlations become negative at the south pole (Amundsen-Scott station). It is also interesting to note that correlation values are exceptionally high between the two CAM5 datasets (original and reconstructed) at Esperanza for all seasons, remaining > 0.80 in DJF and MAM, with values exceeding 0.90 in both JJA and SON.

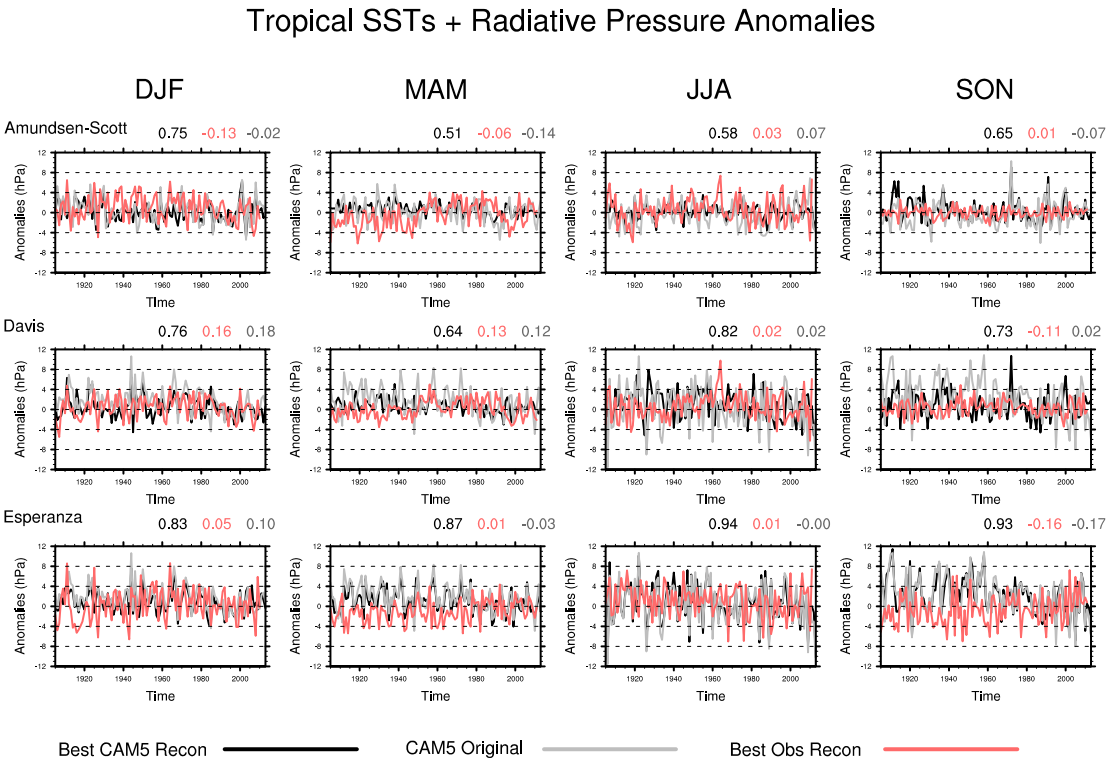

***Figure 3.** Pressure anomaly timeseries of CAM5 best reconstruction (same as from Fig. 2.), CAM5 original data, and the best observational-based reconstruction [1]. Seasonal pressure

anomalies are plotted for 3 different Antarctic stations (gridpoints), including Amundsen-Scott, David and Esperanza. Correlation values between these datasets are also listed at the top of each figure. Values in black represent the correlation between the best CAM5 reconstruction and the original CAM5 dataset, red values indicate the correlation between the best CAM5 reconstruction and the best observational reconstruction, and grey values represent the correlation between the original CAM5 data and the best observational reconstruction. Each value is produced by correlating these datasets over the full time period for each individual station and season.

3.2 Evaluating the Stationarity Constraint

As a means of testing the stationarity of pressure relationships between Antarctica and the southern midlatitudes through time, Figure 4 plots gridpoint correlations around the 15-90°S domain to assess the stability of these relationships throughout the 20th century. These five stations were chosen to provide ample spatial coverage of Antarctica, with correlations broken into two separate time periods that are nearly identical to the calibration and validation periods of our model reconstruction, as well as a difference of the two periods (early – late). The Ozone Only experiment was examined during DJF here as tropospheric ozone forcing is known to have a strong dynamical feedback, with ozone-hole induced cooling of the lower stratosphere leading to a delay in vortex breakdown in the poles [47]. Since the PCR reconstruction method uses southern midlatitude stations to predict pressure at Antarctic stations, the difference plot in the far right hand column helps to dismiss potential uncertainty in the connection between high- and mid-latitude regions. Reconstructions inherently assume stability in relationships through time, which is why we use CAM5 first here to test this assumption.

As previously noted, connections between these regions are driven by large-scale circulation patterns [2,3], and we can see on the difference plot that there are very minute differences through time in the specific locations where the midlatitudes are used as predictors in our reconstructions. The majority of the significant differences (stippling at $p < 0.05$) appear off the west coast of South America, with smaller differences observed elsewhere. Overall, Esperanza exhibits weaker correlations to the midlatitudes in DJF, which was found to be consistent in all CAM5 experiments. Other seasons actually tend to display smaller differences between the two periods and thus keep this stationarity constraint that is assumed by reconstructed data. Even in DJF where ozone forcing has more extensive influence on Antarctic climate and the relationship between the mid- and high-latitudes weakens slightly, southern midlatitude and Antarctica pressure relations still remain stable, providing confidence that relationships established during the early (calibration) period are undoubtedly stationary. In the SSTs + Radiative experiment, there are some significant differences that do appear in JJA between the Antarctic stations and southern midlatitude regions such as South America and parts of southern Africa. However in the SSTs + Fixed Radiative experiment during JJA, these significant differences over land no longer appear, which indicates that tropical SST forcings appear to weaken the relationship between the mid- and high-latitudes, primarily during the winter months.

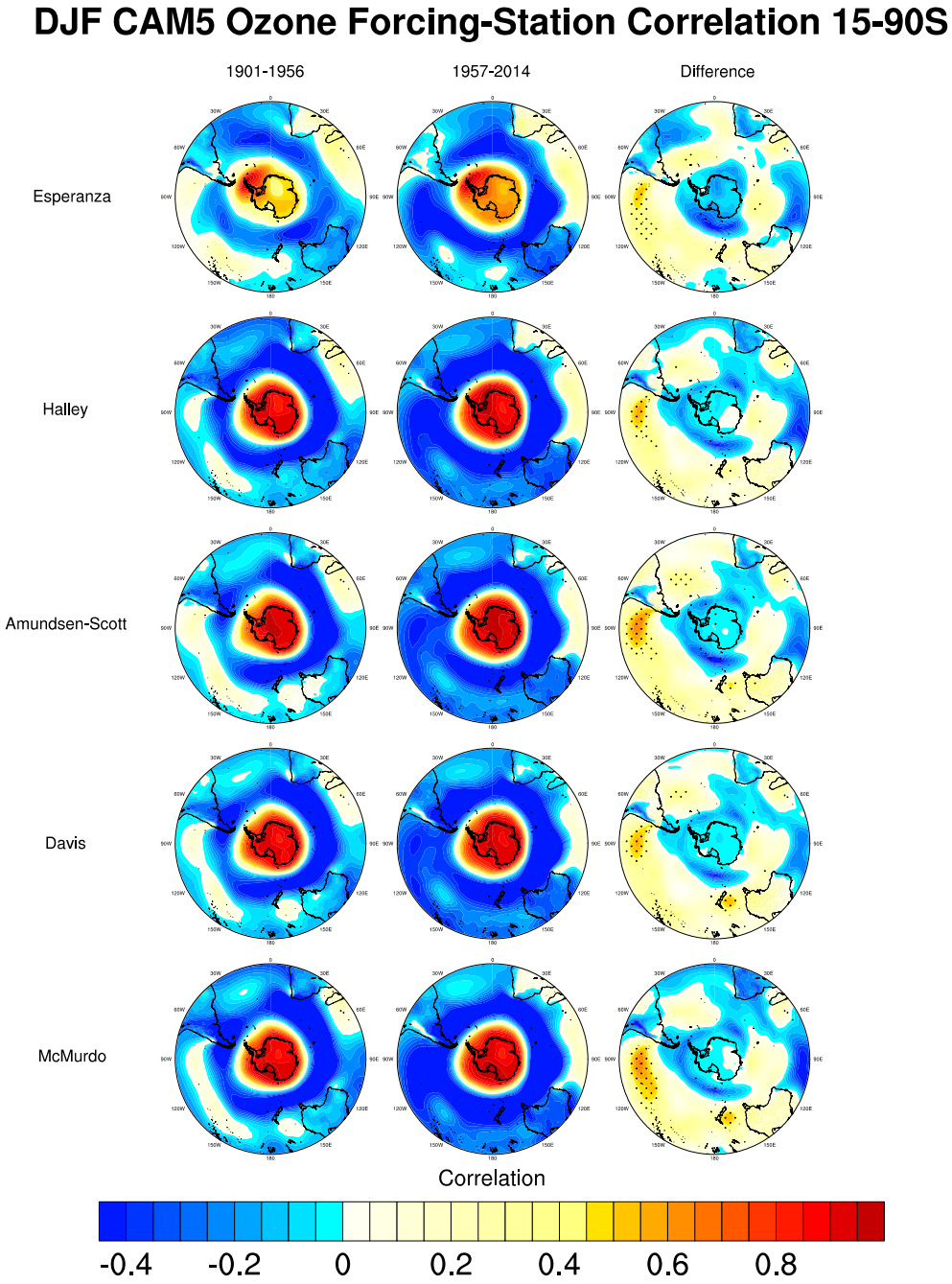

284

285 ***Figure 4.** Station (gridpoint) correlations of 5 locations in Antarctica (i.e. Esperanza, Halley,
286 Amundsen-Scott, Davis and McMurdo) to the surrounding high- and mid-latitudes. Time
287 periods for the 15-90°S correlations include and early period (1901 – 1956), late period (1957 –
288 2014), and a difference of the two (early – late). Stippling on the difference plot indicates
289 regions that are statistically different ($p < 0.05$) from the early period compared to the late
290 period. Ensemble six of the Ozone Only experiment was chosen at random to represent overall
291 CAM5 trends.

292 Century-length global reanalysis products are an essential tool for predicting / understanding
293 climate variability, but have only seen notable improvement in the high latitudes during the latter
294 half of the 20th century with more routinely collected observations [47]. To understand how some of
295 these newer 20th century reanalyses compare to the CAM5 reconstruction, running correlations over
296 30-year periods are plotted in Figure 5 for these reanalyses (also including ERA-Interim), as well as
297 for each CAM5 experiment and 10 ensemble members per simulation. These were area averaged

running correlations between 35 – 60°S (midlatitudes) and 60 – 90°S (high-latitudes) for all datasets, and the CAM5 data were detrended prior to calculating the correlations. As expected, larger discrepancies are shown between CAM5 running correlations and these reanalysis products during the first half of the 20th century. This is shown by the negative correlation values that persist during the full time period in nearly all seasons for CAM5, which is consistent with the strong negative relationships (significant above 1% confidence level) between Antarctica and the 40 - 50°S latitudes [2]. Meanwhile, the century-length reanalyses produce positive, and even some strong positive correlation values ($r > 0.70$) during the first half of the 20th century. ERA-Interim on the other hand appears to match the ensemble members produced by CAM5 during the period of overlap for the 30-year running correlations, showing a high degree of stationarity broadly when comparing these two area-averaged regions. All CAM5 experiments and ensembles remain fairly stable through time, with only ensemble member 2 in MAM appearing to change sign briefly in the early 1940s, which is part of the validation period still. The strong positive correlation values that are depicted by century-length reanalyses during the first half of the 20th century are likely erroneous, as earlier work has noted uncertainty with reanalysis products prior to about 1979 [33]. Thus, further improvement with early 20th century reanalysis products is still needed to provide reliable long-term datasets for pressure.

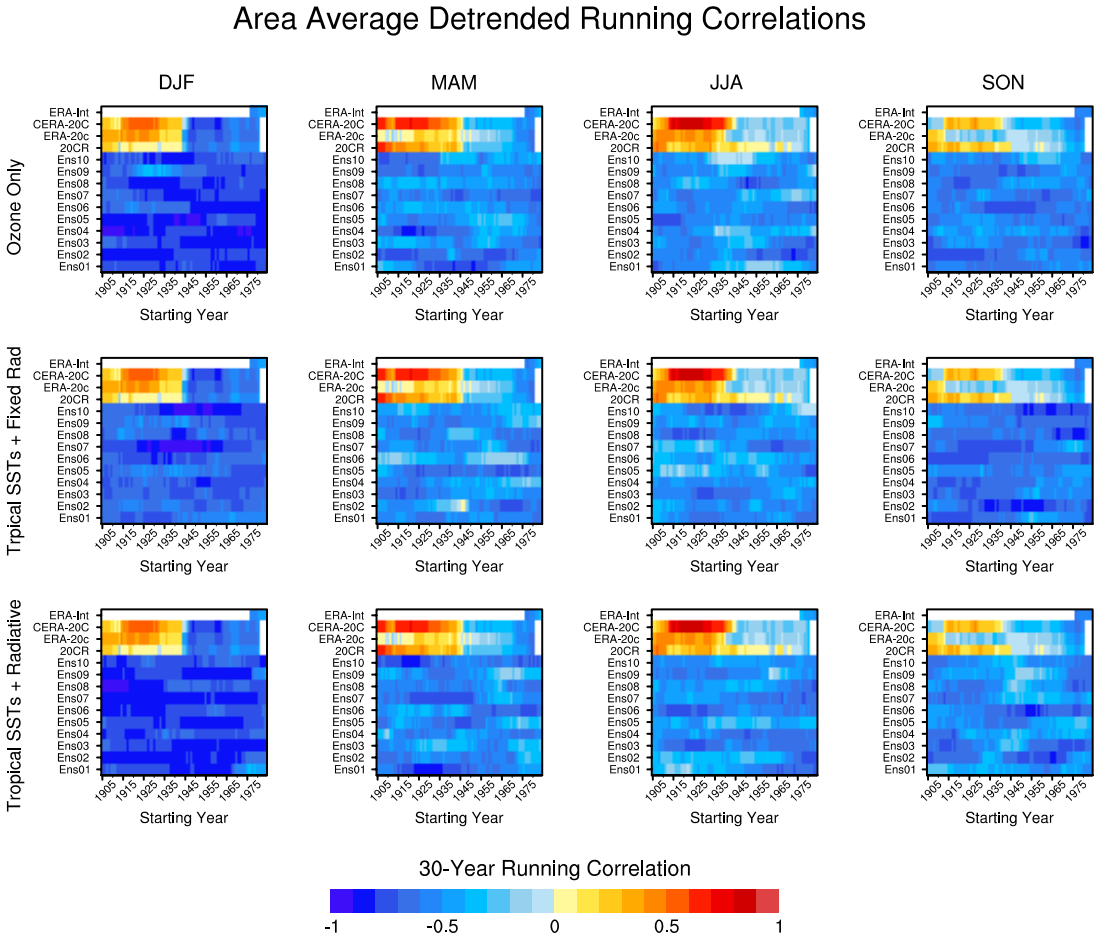

*****Figure 5.** 30-year running correlations between two area-averaged regions (35-60°S and 60-90°S) for CAM5 reconstructions, ERA-Interim, and three century-length reanalyses (CERA-20C, ERA-20C and 20CR). Correlations were done for each CAM5 experiment and 10 ensemble members within each. ERA-Interim doesn't begin until 1976, and the other century-length reanalyses 30-year trends end in 1980. CAM5 data were also detrended prior to generating the reconstruction.

To better understand why these century-length reanalyses produce such large differences when evaluated to the CAM5 reconstructions, a timeseries of the area-averaged pressure anomalies can be found in Figure 6. These are plotted in the first two rows for JJA and MAM, respectively. These seasons were chosen for this figure as the century-length reanalyses produced their strongest positive correlations during in the early half of the 20th century during the months of JJA and MAM, as seen in Fig 5. The third row on Fig. 6 displays the varying correlation magnitude through time, which is done for all seasons. This figure shows how pressure data in the reanalysis products for both the mid and high-latitude regions of the SH has a tendency to behave similarly during the early 20th century, which would explain the strong positive correlation values observed in Fig 5. This behavior in the reanalyses opposes global mass conservation laws and has been a notable issue in the oceans and high-latitudes prior to 1979, where surface pressure in Antarctica was recorded as being anomalously higher and thus contributed to larger global mean pressure values in products like the 40-year ECMWF reanalysis (ERA-40; [48]). This ultimately provides merit in further examining a globally constrained product (i.e. mass field) to examine teleconnections between the mid and high-latitudes in order to explain long-term variability where in situ observations are limited [48]. Near the mid-20th century in Fig. 6, we begin to see the expected pattern of opposite correlations between the mid and high-latitude regions, which would follow expected behavior of pressures covariance structure (i.e. opposite signs) between these two geographical regions, in part reflected in the SAM [2,3,49].

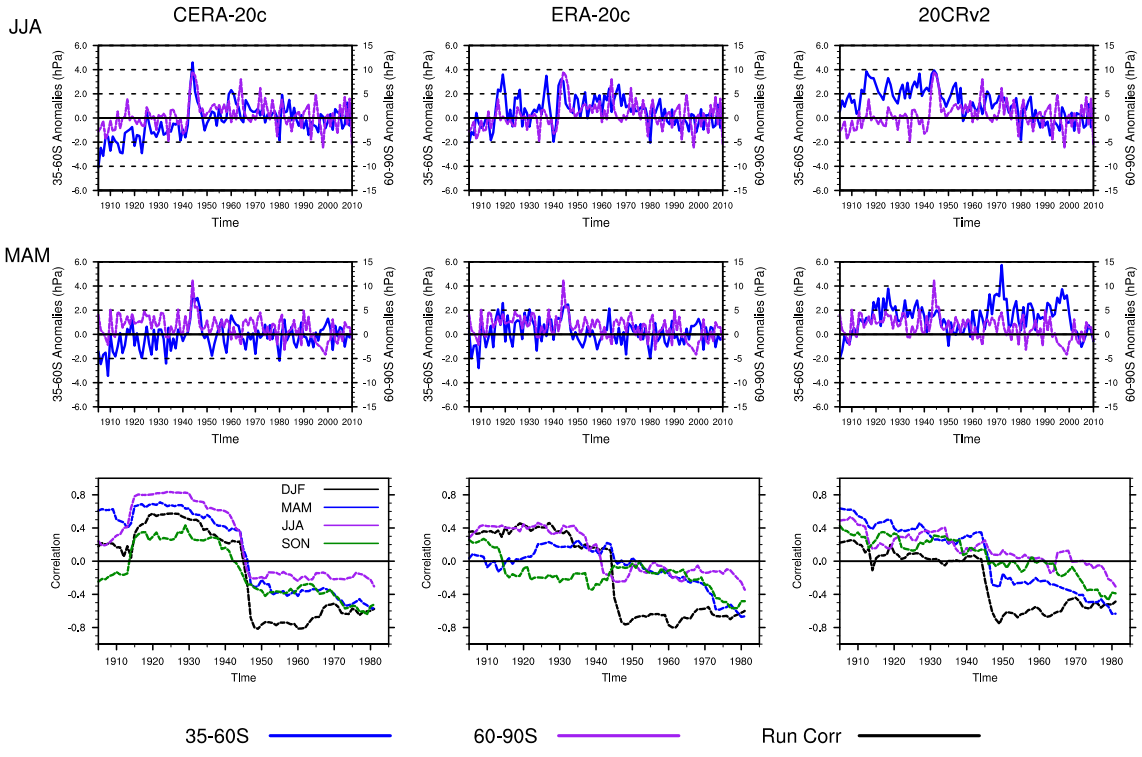

***Figure 6.** The first two rows display seasonal (JJA and MAM) pressure anomalies for the two area-averaged regions (35-60°S and 60-90°S), with different scales on the y-axes for the respective areas. The third row shows all four seasons with their 30-year running correlation values plotted over time. All of these are calculated for the 20th century products of CERA-20c (left column), ERA-20C (middle column) and 20CR (right column).

While these reanalyses continue to show challenges in their utility during the early part of the 20th century, CAM5 can still be evaluated further to understand potential model biases and the role that external forcings might play on shaping Antarctic climate and its connection to the southern midlatitudes. The next step in this process is to reduce the scale and understand how changes are behaving more regionally by examining specific Antarctic stations where the reconstructions were created. By performing PCR to generate our reconstructions, only a subset of southern midlatitude stations were utilized as predictors for Antarctic stations. Figure 7 provides some insight on the number of significantly correlated midlatitude stations ($p < 0.10$) to various Antarctic stations during the 30-year running trend periods. In addition, the solid black line on these plots depicts the number of midlatitude stations used in the Fogt et al. [1] observation-based reconstructions for comparison.

Interestingly, DJF shows that the average of 10 ensemble members in the CAM5 reconstructions all have fewer significantly correlated stations through time when evaluated against the observational reconstruction. This would explain some of the weaker skill that was shown in DJF within the CAM5 model reconstructions (Fig. 2), highlighting a weaker relationships between the mid and high-latitudes during this season. Meanwhile, SON displays the exact opposite in which the model has more significantly correlated midlatitude stations for nearly all 30-year time periods, and thus corresponds to the higher skill previously noted within this season. As such, this indicates that reconstruction skill is highly dependent upon this relationship and the predictor set from the midlatitudes. Throughout some of the other seasons, natural fluctuations occur with the number of significantly correlated stations, but there is no significant change in this relationship over time as suggested by Fig. 4. The stationarity constraint is not violated at the station level in any season except for DJF, and it can be seen from this experiment (Tropical SSTs + Radiative) that the number of significantly correlated midlatitude stations decreases. This decrease in the number of significantly correlated stations holds true in the Tropical SSTs + Fixed Rad during the austral summer, whereas the Ozone Only experiment does not show this decrease, suggesting that tropical SST trends are causing the number of predictors to decrease with time. Therefore, SST forcings appear to have a notable influence on the strength of the relationship between the mid and high-latitudes, slightly weakening the stationarity component in the experiment with time-varying tropical SSTs only, primarily in the summer months.

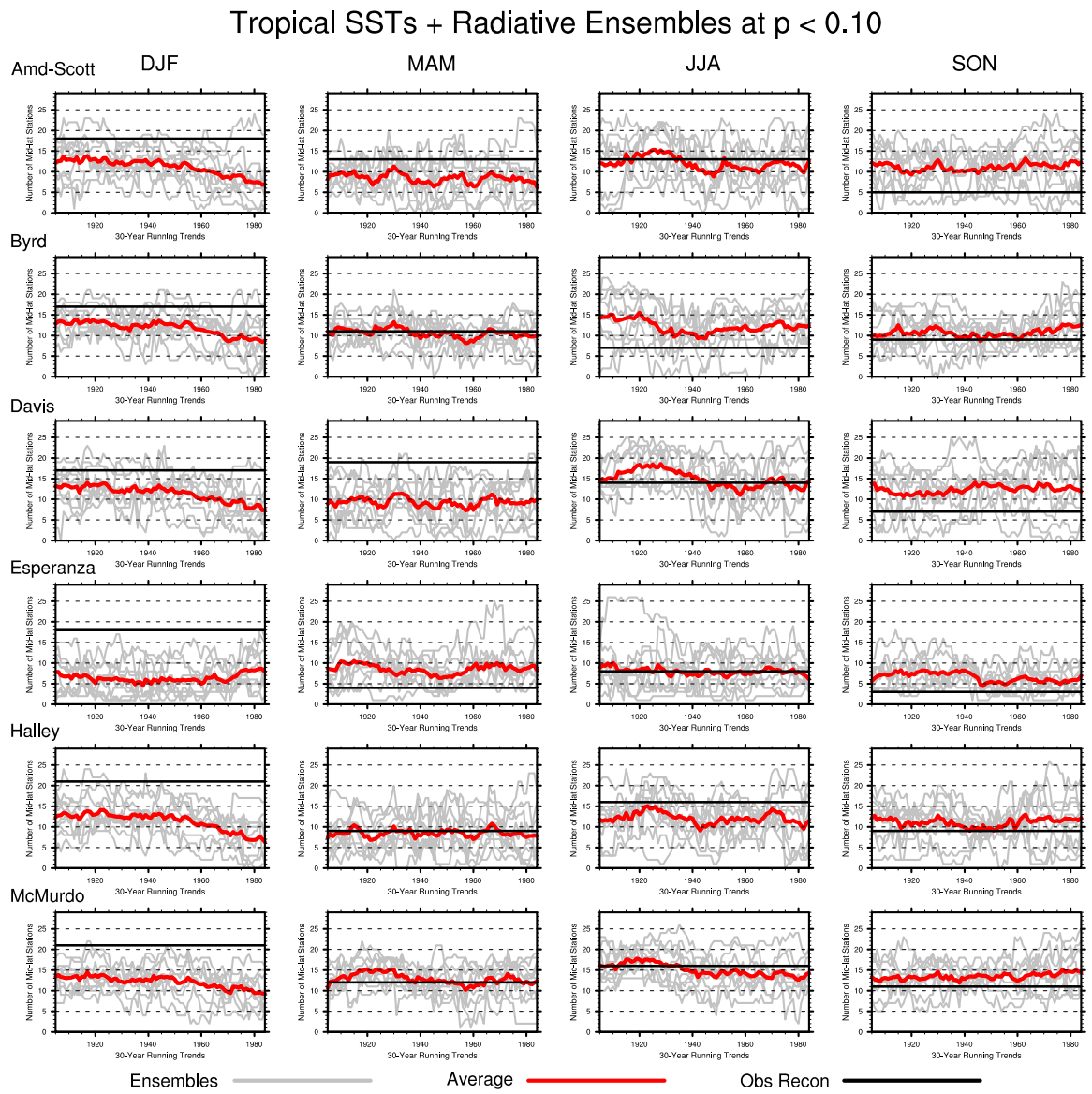

Figure 7. 30-year running trend timeseries of the number of midlatitude stations that are significantly correlated at $p < 0.10$ to Antarctic stations where the reconstructions were generated. The rows account for 6 Antarctic stations that were chosen for display here, including Amundsen-Scott, Byrd, Davis, Esperanza, Halley and McMurdo. For each station and season, 10 ensemble members are plotted from the Tropical SSTs + Radiative CAM5 experiment (grey line), with an average taken from all 10 ensembles (red line), as well as the number of stations that were used in the observational reconstruction (black line) all on each plot.

Another assessment for how the CAM5 model established relationships during the reconstruction period can be shown in Figure 8, in which 30-year running correlations are calculated for all 29 midlatitude stations that were used as the predictors. The SSTs + Radiative experiment was chosen here to represent CAM5, with grouping of stations separated by region indicated by the solid black lines on each plot. In addition, the numbered stations match the names of midlatitude stations previously shown in Fig 1. By grouping the midlatitudes by region, it was shown that there is generally slightly weaker stationarity in the relationships established between Antarctica and locations in Australia, South America the Island stations, where several ensemble members switch sign over the full time period. Even though some ensemble members appear to

violate this stationarity constraint, Fig. 2 still indicates that the overall skill in these CAM5 reconstructions remains fairly high.

The Average Correlation plot in the bottom right helps to provide an overall picture of the CAM5 ensemble mean, which generally remains the same sign (negative correlation) through time, depicting the stationarity once again. The SSTs + Radiative experiment in JJA was chosen as it appeared the most stable through time, which may be due to the fact that varying SSTs and radiational forcings provide a more realistic scenario similar to that which occurs in the real-world. In addition, Fig. 7 showed us that the number of midlatitude stations used for the reconstructions in this season did not have an overall decreasing trend, keeping these relationships more stable through time at the south pole (the farthest latitudinal point from the southern midlatitudes).

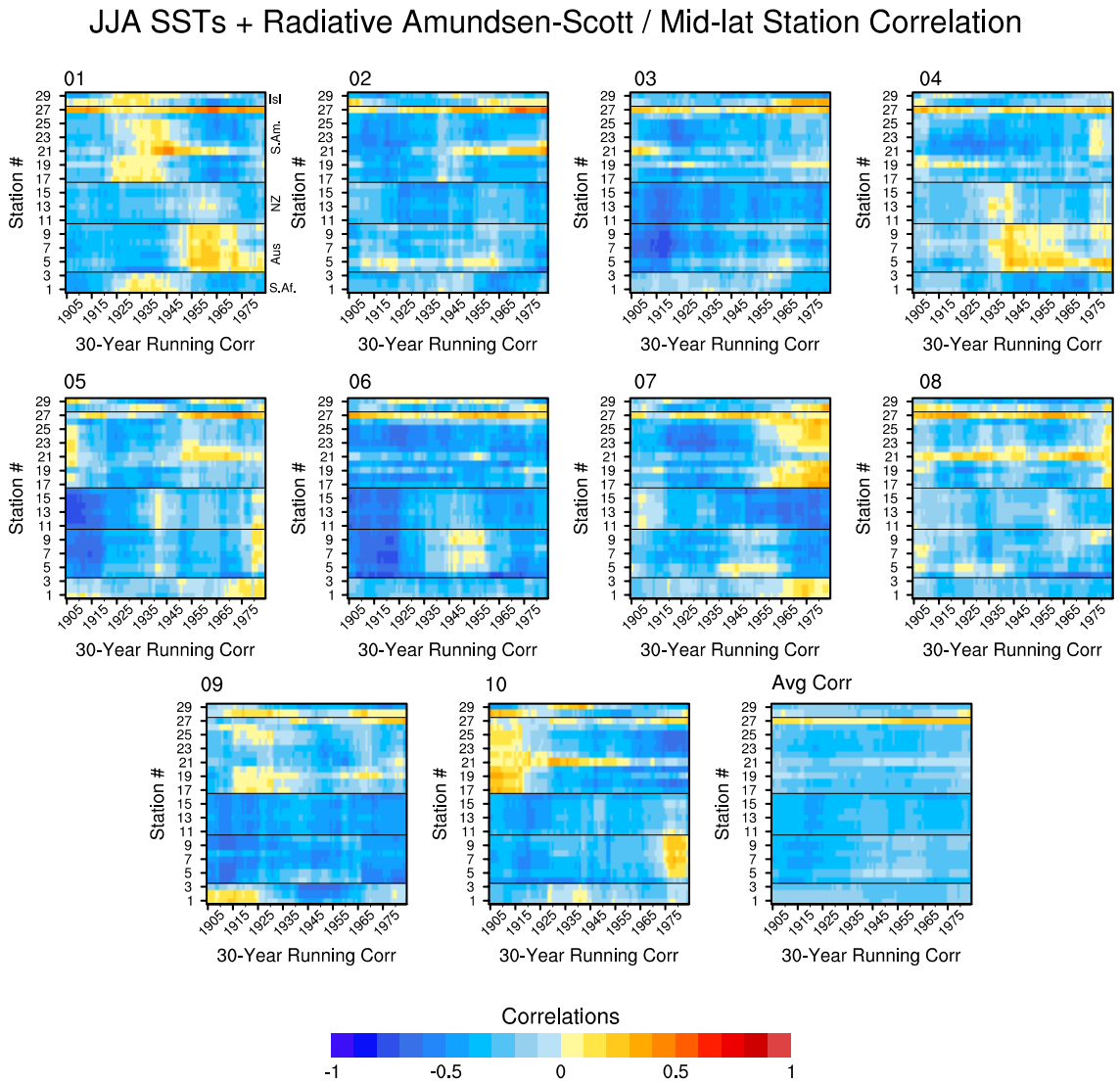

Figure 8. 30-year running correlations across all 29 midlatitude stations to Amundsen-Scott during the austral winter for the SSTs + Radiative CAM5 experiment. All 10 ensemble members, along with an average between these ensembles make up each individual plot. The stations are section off by region, with each number on the y-axis corresponding to the station name listed in Fig 1. The southern midlatitude regions include islands (Isl), South America (S. Am.), New Zealand (NZ), Australia (Aus), and South Africa (S. Af.).

4. Discussion

The primary goal of creating reconstructions is to build an array of new datasets that can be used in the climate realm for understanding long-term atmospheric behavior. This is especially true in the polar-cap regions like Antarctica where meteorological observations remain sparse, presenting the need for more long-term, and reliable datasets. The goal of using CAM5 to generate reconstructions was to not only verify the stationarity constraint that is inherently assumed in reconstructed datasets, but to also provide a new perspective on how a model, with the ability to isolate external forcings, behaves in recreating long-term pressure. When evaluated to the best observational reconstruction [1] in Fig. 2, our modeled reconstructions recorded higher skill metrics in all seasons with the exception of DJF. However, the timeseries in Fig. 3 displayed some of the marked anomalous pressure that is in the original CAM5 dataset compared to the obs recon, which would lead to some erroneous data in CAM5 reconstructions. Comparing the CAM5 reconstructions to reanalysis products, the biggest theme was that reanalyses produced anomalously high correlation values in the first half of the 20th century, which differs than the expected negative correlations when comparing pressure between Antarctica and the southern midlatitudes (based on the mass conservation law). Overall, it appeared that the SSTs + Radiative experiment with CAM5 proved to be most stationary and had higher skill metrics for SON and MAM when compared to the observation-based reconstruction, whereas the Ozone only forcing generally had the highest calibration reconstruction skill in DJF and JJA. It was found that the SSTs + Radiative, along with the SSTs + Fixed Radiative experiments in CAM5 had a notable decrease in the number of significantly correlated midlatitude stations used as predictors in DJF, which weakened the overall skill in the summer season. Thus, the number of predictors used to generate reconstructions based on the PCR methodology has a significant influence on overall reconstruction skill. Based on the overall results found here, the stationarity constraint assumed between the mid and high-latitudes does remain fairly stable through time, which allows us to create reconstructions solely based on the relationship between these two regions. Identifying stationarity in these relationships is imperative for the creating these pressure reconstructions, gaining more confidence in their reliability in understanding long-term climate variability, and ultimately assisting in the validation of models that predict the future state of the climate.

Supplementary Materials: The following are available online at www.mdpi.com/xxx/s1, Figure S1: title, Table S1: title, Video S1: title.

Author Contributions: For research articles with several authors, a short paragraph specifying their individual contributions must be provided. The following statements should be used "conceptualization, X.X. and Y.Y.; methodology, X.X.; software, X.X.; validation, X.X., Y.Y. and Z.Z.; formal analysis, X.X.; investigation, X.X.; resources, X.X.; data curation, X.X.; writing—original draft preparation, X.X.; writing—review and editing, X.X.; visualization, X.X.; supervision, X.X.; project administration, X.X.; funding acquisition, Y.Y.", please turn to the CRediT taxonomy for the term explanation. Authorship must be limited to those who have contributed substantially to the work reported.

Funding: Please add: "This research received no external funding" or "This research was funded by NAME OF FUNDER, grant number XXX" and "The APC was funded by XXX". Check carefully that the details given are accurate and use the standard spelling of funding agency names at https://search.crossref.org/funding, any errors may affect your future funding.

Acknowledgments: In this section you can acknowledge any support given which is not covered by the author contribution or funding sections. This may include administrative and technical support, or donations in kind (e.g., materials used for experiments).

Conflicts of Interest: Declare conflicts of interest or state "The authors declare no conflict of interest." Authors must identify and declare any personal circumstances or interest that may be perceived as inappropriately influencing the representation or interpretation of reported research results. Any role of the funders in the design of the study; in the collection, analyses or interpretation of data; in the writing of the manuscript, or in the decision to publish the results must be declared in this section. If there is no role, please state "The funders had

no role in the design of the study; in the collection, analyses, or interpretation of data; in the writing of the manuscript, or in the decision to publish the results".

Appendix A

The appendix is an optional section that can contain details and data supplemental to the main text. For example, explanations of experimental details that would disrupt the flow of the main text, but nonetheless remain crucial to understanding and reproducing the research shown; figures of replicates for experiments of which representative data is shown in the main text can be added here if brief, or as Supplementary data. Mathematical proofs of results not central to the paper can be added as an appendix.

References

1. Fogt, R.L.; Goergens, C.A.; Jones, M.E.; Witte, G.A.; Lee, M.Y.; Jones, J.M. Antarctic station-based seasonal pressure reconstructions since 1905: 1. Reconstruction evaluation: Antarctic Pressure Evaluation. *J. Geophys. Res. Atmospheres* **2016**, *121*, 2814–2835.
2. Gong, D.; Wang, S. Definition of Antarctic Oscillation index. *Geophys. Res. Lett.* **1999**, *26*, 459–462.
3. Thompson, D.W.J.; Wallace, J.M. Annular Modes in the Extratropical Circulation. Part I: Month-to-Month Variability*. *J. Clim.* **2000**, *13*, 1000–1016.
4. Gallego, D.; Ribera, P.; Garcia-Herrera, R.; Hernandez, E.; Gimeno, L. A new look for the Southern Hemisphere jet stream. *Clim. Dyn.* **2005**, *24*, 607–621.
5. Rogers, J.C.; van Loon, H. Spatial Variability of Sea Level Pressure and 500 mb Height Anomalies over the Southern Hemisphere. *Mon. Weather Rev.* **1982**, *110*, 1375–1392.
6. Marshall, G.J. Half-century seasonal relationships between the Southern Annular mode and Antarctic temperatures. *Int. J. Climatol.* **2007**, *27*, 373–383.
7. Baldwin, M.P. Annular modes in global daily surface pressure. *Geophys. Res. Lett.* **2001**, *28*, 4115–4118.
8. Kidson, J.W. Principal Modes of Southern Hemisphere Low-Frequency Variability Obtained from NCEP–NCAR Reanalyses. *J. Clim.* **1999**, *12*, 2808–2830.
9. Trenberth, K.E. The Definition of El Niño. *Bull. Am. Meteorol. Soc.* **1997**, *78*, 2771–2777.
10. Mantua, N.J.; Hare, S.R. The Pacific Decadal Oscillation. *J. Oceanogr.* **2002**, *58*, 35–44.
11. Henley, B.J.; Gergis, J.; Karoly, D.J.; Power, S.; Kennedy, J.; Folland, C.K. A Tripole Index for the Interdecadal Pacific Oscillation. *Clim. Dyn.* **2015**, *45*, 3077–3090.
12. Enfield, D.B.; Mestas-Nuñez, A.M.; Trimble, P.J. The Atlantic Multidecadal Oscillation and its relation to rainfall and river flows in the continental U.S. *Geophys. Res. Lett.* **2001**, *28*, 2077–2080.
13. Revell, M.J.; Kidson, J.W.; Kiladis, G.N. Interpreting Low-Frequency Modes of Southern Hemisphere Atmospheric Variability as the Rotational Response to Divergent Forcing. *Mon. Weather Rev.* **2001**, *129*, 2416–2425.
14. Turner, J. The El Niño–southern oscillation and Antarctica. *Int. J. Climatol.* **2004**, *24*, 1–31.

15. Lachlan-Cope, T.; Connolley, W. Teleconnections between the tropical Pacific and the Amundsen-Bellinghausens Sea: Role of the El Niño/Southern Oscillation. *J. Geophys. Res. Atmospheres* **2006**, *111*, n/a-n/a.
16. Clem, K.R.; Fogt, R.L. South Pacific circulation changes and their connection to the tropics and regional Antarctic warming in austral spring, 1979-2012: S. Pacific Trends and Tropical Influence. *J. Geophys. Res. Atmospheres* **2015**, *120*, 2773–2792.
17. Meehl, G.A.; Arblaster, J.M.; Bitz, C.M.; Chung, C.T.Y.; Teng, H. Antarctic sea-ice expansion between 2000 and 2014 driven by tropical Pacific decadal climate variability. *Nat. Geosci.* **2016**, *9*, 590–595.
18. Purich, A.; England, M.H.; Cai, W.; Chikamoto, Y.; Timmermann, A.; Fyfe, J.C.; Frankcombe, L.; Meehl, G.A.; Arblaster, J.M. Tropical Pacific SST Drivers of Recent Antarctic Sea Ice Trends. *J. Clim.* **2016**, *29*, 8931–8948.
19. Li, X.; Holland, D.M.; Gerber, E.P.; Yoo, C. Impacts of the north and tropical Atlantic Ocean on the Antarctic Peninsula and sea ice. *Nature* **2014**, *505*, 538–542.
20. L'Heureux, M.L.; Thompson, D.W.J. Observed Relationships between the El Niño–Southern Oscillation and the Extratropical Zonal-Mean Circulation. *J. Clim.* **2006**, *19*, 276–287.
21. Fogt, R.L.; Bromwich, D.H.; Hines, K.M. Understanding the SAM influence on the South Pacific ENSO teleconnection. *Clim. Dyn.* **2011**, *36*, 1555–1576.
22. Wilson, A.B.; Bromwich, D.H.; Hines, K.M. Simulating the Mutual Forcing of Anomalous High Southern Latitude Atmospheric Circulation by El Niño Flavors and the Southern Annular Mode. *J. Clim.* **2016**, *29*, 2291–2309.
23. Gong, T.; Feldstein, S.B.; Luo, D. The Impact of ENSO on Wave Breaking and Southern Annular Mode Events. *J. Atmospheric Sci.* **2010**, *67*, 2854–2870.
24. Gong, T.; Feldstein, S.B.; Luo, D. A Simple GCM Study on the Relationship between ENSO and the Southern Annular Mode. *J. Atmospheric Sci.* **2013**, *70*, 1821–1832.
25. Yiu, Y.Y.S.; Maycock, A.C. On the seasonality of the El Niño teleconnection to the Amundsen Sea region. *J. Clim.* **2019**.
26. Jones, J.M.; Widmann, M. Early peak in Antarctic oscillation index. *Nature* **2004**, *432*, 290–291.
27. Jones, J.M.; Fogt, R.L.; Widmann, M.; Marshall, G.J.; Jones, P.D.; Visbeck, M. Historical SAM Variability. Part I: Century-Length Seasonal Reconstructions*. *J. Clim.* **2009**, *22*, 5319–5345.
28. Visbeck, M. A Station-Based Southern Annular Mode Index from 1884 to 2005. *J. Clim.* **2009**, *22*, 940–950.
29. Fogt, R.L.; Jones, J.M.; Goergens, C.A.; Jones, M.E.; Witte, G.A.; Lee, M.Y. Antarctic station-based seasonal pressure reconstructions since 1905: 2. Variability and trends during the twentieth century: ANTARCTIC PRESSURE RECONSTRUCTION TRENDS. *J. Geophys. Res. Atmospheres* **2016**, *121*, 2836–2856.
30. Mann, M.E. Climate Over the Past Two Millennia. *Annu. Rev. Earth Planet. Sci.* **2007**, *35*, 111–136.

31. Marshall, G.J.; Bracegirdle, T.J. An examination of the relationship between the Southern Annular Mode and Antarctic surface air temperatures in the CMIP5 historical runs. *Clim. Dyn.* **2015**, *45*, 1513–1535.
32. Hosking, J.S.; Orr, A.; Marshall, G.J.; Turner, J.; Phillips, T. The Influence of the Amundsen–Bellingshausen Seas Low on the Climate of West Antarctica and Its Representation in Coupled Climate Model Simulations. *J. Clim.* **2013**, *26*, 6633–6648.
33. Fogt, R.L.; Goergens, C.A.; Jones, J.M.; Schneider, D.P.; Nicolas, J.P.; Bromwich, D.H.; Dusselier, H.E. A twentieth century perspective on summer Antarctic pressure change and variability and contributions from tropical SSTs and ozone depletion. *Geophys. Res. Lett.* **2017**, *44*, 9918–9927.
34. Fogt, R.L.; Schneider, D.P.; Goergens, C.A.; Jones, J.M.; Clark, L.N.; Garberoglio, M.J. Seasonal Antarctic pressure variability during the twentieth century from spatially complete reconstructions and CAM5 simulations. *Clim. Dyn.* **2019**.
35. Turner, J.; Bracegirdle, T.J.; Phillips, T.; Marshall, G.J.; Hosking, J.S. An Initial Assessment of Antarctic Sea Ice Extent in the CMIP5 Models. *J. Clim.* **2013**, *26*, 1473–1484.
36. Jones, J.M.; Gille, S.T.; Goosse, H.; Abram, N.J.; Canziani, P.O.; Charman, D.J.; Clem, K.R.; Crosta, X.; de Lavergne, C.; Eisenman, I.; et al. Assessing recent trends in high-latitude Southern Hemisphere surface climate. *Nat. Clim. Change* **2016**, *6*, 917–926.
37. Bracegirdle, T.J.; Colleoni, F.; Abram, N.J.; Bertler, N.A.N.; Dixon, D.A.; England, M.; Favier, V.; Fogwill, C.J.; Fyfe, J.C.; Goodwin, I.; et al. Back to the Future: Using Long-Term Observational and Paleo-Proxy Reconstructions to Improve Model Projections of Antarctic Climate. *Geosciences* **2019**, *9*, 255.
38. Schneider, D.P.; Fogt, R.L. Artifacts in Century-Length Atmospheric and Coupled Reanalyses Over Antarctica Due To Historical Data Availability. *Geophys. Res. Lett.* **2018**, *45*, 964–973.
39. Fogt, R.L.; Clark, L.N.; Nicolas, J.P. A New Monthly Pressure Dataset Poleward of 60°S since 1957. *J. Clim.* **2018**, *31*, 3865–3874.
40. Compo, G.P.; Whitaker, J.S.; Sardeshmukh, P.D.; Matsui, N.; Allan, R.J.; Yin, X.; Gleason, B.E.; Vose, R.S.; Rutledge, G.; Bessemoulin, P.; et al. The Twentieth Century Reanalysis Project. *Q. J. R. Meteorol. Soc.* **2011**, *137*, 1–28.
41. Poli, P.; Hersbach, H.; Dee, D.P.; Berrisford, P.; Simmons, A.J.; Vitart, F.; Laloyaux, P.; Tan, D.G.H.; Peubey, C.; Thépaut, J.-N.; et al. ERA-20C: An Atmospheric Reanalysis of the Twentieth Century. *J. Clim.* **2016**, *29*, 4083–4097.
42. Laloyaux, P.; Thépaut, J.-N.; Dee, D. Impact of Scatterometer Surface Wind Data in the ECMWF Coupled Assimilation System. *Mon. Weather Rev.* **2016**, *144*, 1203–1217.
43. Cram, T.A.; Compo, G.P.; Yin, X.; Allan, R.J.; McColl, C.; Vose, R.S.; Whitaker, J.S.; Matsui, N.; Ashcroft, L.; Auchmann, R.; et al. The International Surface Pressure Databank version 2. *Geosci. Data J.* **2015**, *2*, 31–46.
44. Woodruff, S.D.; Worley, S.J.; Lubker, S.J.; Ji, Z.; Eric Freeman, J.; Berry, D.I.; Brohan, P.; Kent, E.C.; Reynolds, R.W.; Smith, S.R.; et al. ICOADS Release 2.5: extensions and enhancements to the surface marine meteorological archive. *Int. J. Climatol.* **2011**, *31*, 951–967.

590 45. Bromwich, D.H.; Nicolas, J.P.; Monaghan, A.J. An Assessment of Precipitation Changes
591 over Antarctica and the Southern Ocean since 1989 in Contemporary Global Reanalyses
592 *. *J. Clim.* **2011**, *24*, 4189–4209.
593 46. Bracegirdle, T.J.; Marshall, G.J. The Reliability of Antarctic Tropospheric Pressure and
594 Temperature in the Latest Global Reanalyses. *J. Clim.* **2012**, *25*, 7138–7146.
595 47. Stolarski, R.S.; Douglass, A.R.; Gupta, M.; Newman, P.A.; Pawson, S.; Schoeberl, M.R.;
596 Nielsen, J.E. An ozone increase in the Antarctic summer stratosphere: A dynamical
597 response to the ozone hole. *Geophys. Res. Lett.* **2006**, *33*.
598 48. Trenberth, K.E.; Smith, L. The Mass of the Atmosphere: A Constraint on Global
599 Analyses. *J. Clim.* **2005**, *18*, 864–875.
600 49. Marshall, G.J. Trends in the southern annular mode from observations and reanalyses. *J.*
601 *Clim.* **2003**, *16*, 4134–4143.
602

603